Estuarine, Coastal and Shelf Science (1995) **40,** 529–544

Entrainment of Nitrate in the Fraser River Estuary and its Biological Implications. II. Effects of Spring *vs*. Neap Tides and River Discharge

Kedong Yin[a], Paul J. Harrison[a], Stephen Pond[a] and Richard J. Beamish[b]

[a]*Department of Oceanography, University of British Columbia, Vancouver, British Columbia, V6T 1Z4 Canada and* [b]*Pacific Biological Station, Department of Fisheries and Oceans, Nanaimo, British Columbia, V9R 5K6 Canada*

Received 2 December 1992 and in revised form 14 April 1994

Keywords: nitrate entrainment; riverine plume; estuarine plume; spring tide; neap tide; river discharge; Fraser River; Strait of Georgia

A 24-h time series of high-resolution vertical profiles of salinity, temperature, NO_3 and fluorescence were taken during spring and neap tides at an anchored station (station 2) in the Strait of Georgia, 8 km seaward of the mouth of the Fraser River in order to estimate entrainment of NO_3 resulting from the outflowing riverine plume. The time series confirmed that more NO_3 was entrained during the spring tide (24 mmol m^{-2}) than during the neap tide (17 mmol m^{-2}). The contribution of the entrained NO_3 was 2·3 and 1·6 times that of the river-borne NO_3 during spring and neap tides, respectively. We hypothesize that spring tides cause stronger bottom stirring which results in higher NO_3 concentrations in the deep seawater which is the source of NO_3 that is entrained upward. The results from the times series taken during days of different river discharge show that during higher river discharge (9000 m^3 s^{-1}) more NO_3 (72 mmol m^{-2}) was entrained than during lower (6720 m^3 s^{-1}) river discharge (32 mmol m^{-2}). The entrained NO_3 was 5·4 times that of the river-borne NO_3 during the higher river discharge and 3·3 times during the lower discharge. The mechanism which explains the greater NO_3 entrainment is that greater river discharge pushes the estuarine plume seaward, further from the river mouth, and therefore there is a larger area of deep seawater (with higher NO_3 concentrations) exposed directly to the riverine plume for entrainment.

Introduction

Entrainment of nutrients becomes very important when the nutrient concentrations of the river are lower than the receiving seawater in the estuary. This is the case for the Fraser River estuary and the adjacent region of the Strait of Georgia. The magnitude of annual primary production has been debated for the Strait of Georgia. Stockner *et al.*'s (1979) estimate on annual primary production is three times higher than Parsons *et al.*'s

0272–7714/95/050529+16 $08.00/0

(1970) estimate. Stockner *et al.* (1979) attributed the increase in annual primary production to eutrophication produced by the nutrients in the Fraser River runoff. However, the nutrient (nitrate) data in the Fraser River for the same period as their study (Drinnan & Clark, 1980) did not support this argument. In the subsequent discussion, entrainment of nutrients (nitrate) due to the Fraser River discharge was proposed to be a major process that could supply nitrate and satisfy the nitrogen budget requirement for the increase in annual primary production estimated by Stockner *et al.* (1979; Parsons *et al.*, 1980; Harrison *et al.*, 1983). Entrainment of nitrate is believed to be particularly important in late spring and summer when nitrogen is undetectable in the estuarine plume in the Strait and the Fraser River carries concentrations of NO_3 as low as 2 μM, the minimum for the year in September (Drinnan & Clark, 1980).

In spite of frequently undetectable concentrations of NO_3 in the estuarine plume, primary production remains high during the annual freshet (June and July) (Clifford *et al.*, 1989, 1990, 1991). Recent evidence indicates that the regions of higher productivity were found to occur at stations in the estuarine plume some distance away from the Fraser River (Clifford *et al.*, 1991). A phytoplankton bloom was observed during pre-neap tides in July in the estuarine plume (Harrison *et al.*, 1991). This high production cannot be explained by the nutrient input from the river outflow alone, because NO_3 concentrations in the river in late spring and summer add only 2–6 μM. In addition, surface nutrients are diluted when the riverine plume flows over and entrains the nutrient-depleted estuarine plume (Yin *et al.*, 1995*a*). These observations point to the entrainment of NO_3 as being partially responsible for the higher productivity.

Two plumes are present in the vicinity of the Fraser River estuary: the riverine plume and the estuarine plume (Harrison *et al.*, 1991; Yin *et al.*, 1995*a*). A new riverine plume is formed by the river outflow, particularly during ebb tides. When old riverine plumes mix with seawater and remain in the Strait of Georgia, they form a stratified layer referred to as the estuarine plume. Thus, the riverine plume usually spreads over the estuarine plume. Nitrate concentrations are usually very low or undetectable in the estuarine plume in late spring and summer. In a previous study (Yin *et al.*, 1995*a*), the estuarine plume was found to invade the river with the advance of the salt wedge on flood tides and to form a barrier which hinders direct mixing between the freshwater and the deep water. Upward entrainment of high NO_3 into the riverine plume occurs during ebb tides only when the NO_3-poor estuarine plume is pushed seaward, allowing the riverine plume to come into contact with the deep NO_3-rich seawater (see Figure 3 in Yin *et al.*, 1995*a*). Therefore, the amount of the entrained NO_3 depends on the amount of the entrained deep water, which varies with tidal cycles. There is more direct contact between the freshwater and the deep water during a spring tide when the estuarine plume is flushed out of the river, suggesting more NO_3 entrainment during a spring tide than during a neap tide. The mechanisms could be two-fold; spring tides result in strong mixing and hence, high NO_3 concentrations in the deep water near the river mouth; and lower low water during spring tides results in more freshwater outflow than during other tides and stronger current shears during the outflow. Similarly, as the river discharge increases, more entrainment of NO_3 is possible.

The objectives of this study were to examine the effects of tides (spring/neap) and river discharge on entrainment and to estimate entrained NO_3 over a diurnal tidal cycle, and to determine the relationship between the amount of the entrained deep water and entrained NO_3. In the next study, we will examine the effects of winds on entrainment of NO_3 (Yin *et al.*, 1995*b*).

Materials and methods

A map of the study area is given in the previous paper (see Figure 4 in Yin *et al.*, 1995*a*). Station 2 is 8 km seaward of the mouth of the Fraser River (where the river leaves the edge of the banks). Continuous vertical profiles of temperature, salinity, *in vivo* fluorescence and NO_3 were obtained as described in the previous paper (Yin *et al.*, 1995*a*). Vertical profiles were taken every 2–4 h for 24 h at station 2 while the ship was anchored. Four time series were made under different conditions: during a spring tide and neap tide (under similar magnitudes of river discharge) in June 1989 and during different amounts of river discharge at the end of May (lower discharge) and early June 1990 (higher discharge).

Contour plots of salinity and NO_3 were made with a computer program (Surfer). Owing to the multi-layered water column, the vertical distribution of NO_3 showed lower concentrations at an intermediate depth than at the surface, or a minimum or even two minima in a profile. Such NO_3 distributions have made the contour plots in Figure 1(b,d) and Figure 4(b,d) look complex. The interpretation of these plots is supported by individual profiles (not shown). The time used in all the contour plots is local time (PST).

Temperature–salinity (T-S) diagrams were used for calculating the equivalent thickness of freshwater, the estuarine plume (EP), the entrained estuarine plume (EEP), the entrained deep water (EDW), and the amount of entrained NO_3 as well as integrated fluorescence contributed by the estuarine plume (Int. Flu.). The calculation procedures were described in the previous study (Yin *et al.*, 1995*a*).

Results

Because of the Coriolis effect, the riverine plume tends to turn to the north as it enters the Strait. Station 2 is normally in the path of the riverine plume, but depending on winds, it is possible for the riverine plume to move north or south of station 2 if winds blow strongly enough to the north or south. The river outflow reaches a maximum near lower low water (LLW) at the river mouth. There is a time lag for the riverine plume to arrive at station 2. This time lag of a few hours was observed during the time series.

Effects of tides on entrainment

Neap tide

Surface salinities were <10 during the two floods and >14 during the ebb tides, indicating that the riverine plume was blocked for some time by the flood and reached station 2 some time after ebb tide [Figure 1(a)]. The salinity of 28 can be considered to represent the bottom boundary of the upper stratified layer: the estuarine plume. Its depth fluctuated between 10 and 14 m, rising as higher high water (HHW) was approached [Figure 1(a)]. The gradients in the isohalines were greater during tidal flooding when the surface salinity was lower [Figure 1(a)].

The time series of T-S diagrams in Figure 2(a) show that there were more than two water masses and the T-S curves changed over time. The riverine plume was identified by lower salinities (<15) and temperature; the estuarine plume was generally characterized by medium salinities (20–27) and higher temperatures than the river, and the transition to the deep seawater was represented by the steep straight line segment to the

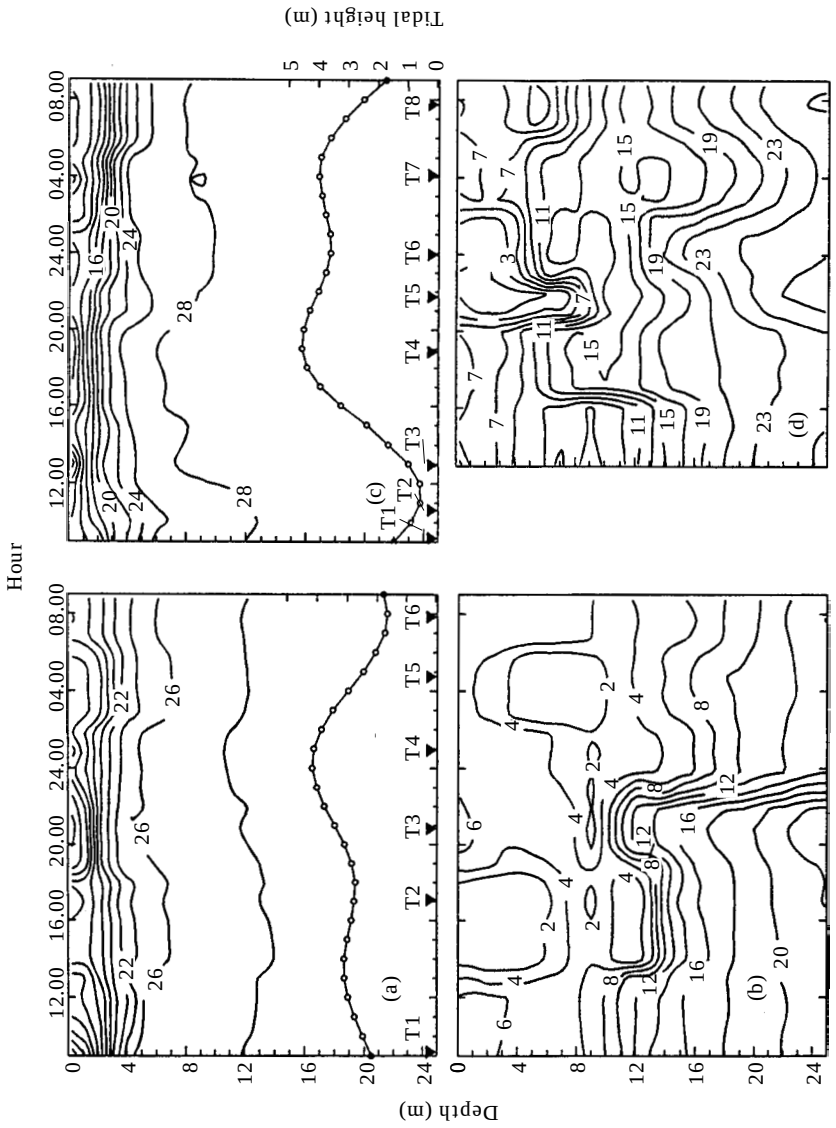

Figure 1. Depth contours of (a,c) salinity and (b,d) NO_3 (μM) for the time series at station 2 on 12–13 June during the neap tide (a,b) and 19–20 June 1989 during the spring tide (c,d). The arrows indicate the times when the vertical profiles were completed since it usually took 0·5 h to complete a vertical profile.

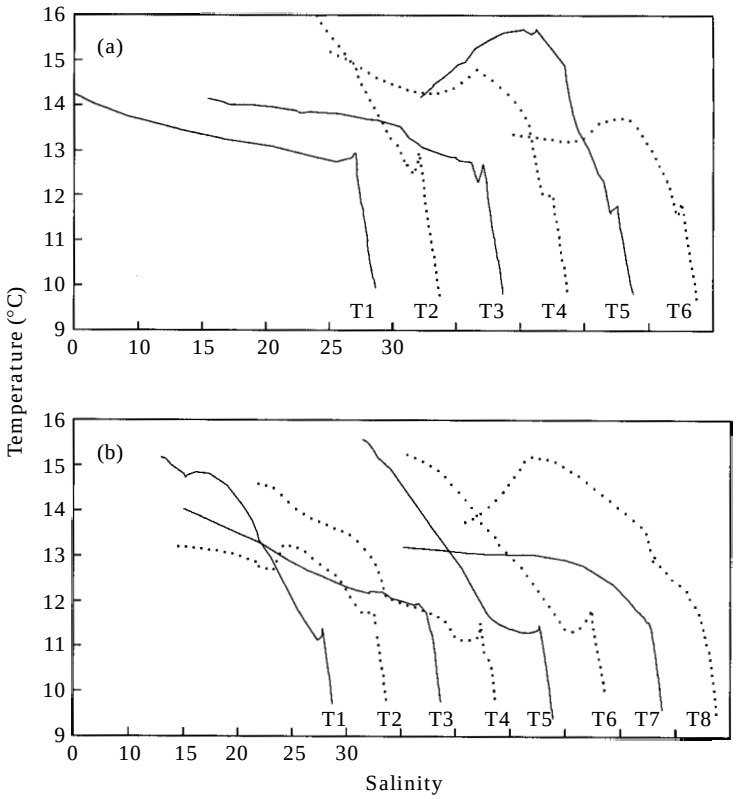

Figure 2. Time series of the T-S diagrams for (a) the neap tide and (b) the spring tide. See Figure 1(a) for the sampling times and their relation to the tidal cycles. Successive T-S curves are offset by 5 on the salinity axis.

right of salinity 27. Since the temperature of freshwater changed little over a tidal cycle, it was the temperature of the estuarine plume that changed most dramatically due to mixing with the riverine plume or the deep water during a tidal cycle. For example, at T1, 2 h after LLW, the riverine plume dominated while at T2 the estuarine plume was dominant. At T4 and T6, the temperature of the riverine plume decreased with salinity (the left part of the T-S curve) and then rose at intermediate salinities (15–20) [Figure 2(a)], indicating mixing with water which was colder than the surface estuarine plume. The mixture with the colder water in the riverine plume must have resulted from entrainment of the deep water. An interesting feature that was consistently present in each of the T-S diagrams was the little kink at about salinity 27, which often separated the two line segments with distinctly different slopes on each side. The lines to the right of the kink represent the mixing lines between the estuarine plume and the deep seawater and the slopes were steep, indicating a rapidly increasing temperature with decreasing salinity. The curves to the left changed over the tidal cycle. The kink might be due to entrainment of the deep seawater into the estuarine plume at their interface. The kink may be expanded when entrainment increases.

The surface NO_3 concentrations were abut 6–7 μM when the surface salinity was low (09.00–12.00h), and very low (2 μM) from 14.00 to 18.00h when the salinity was higher

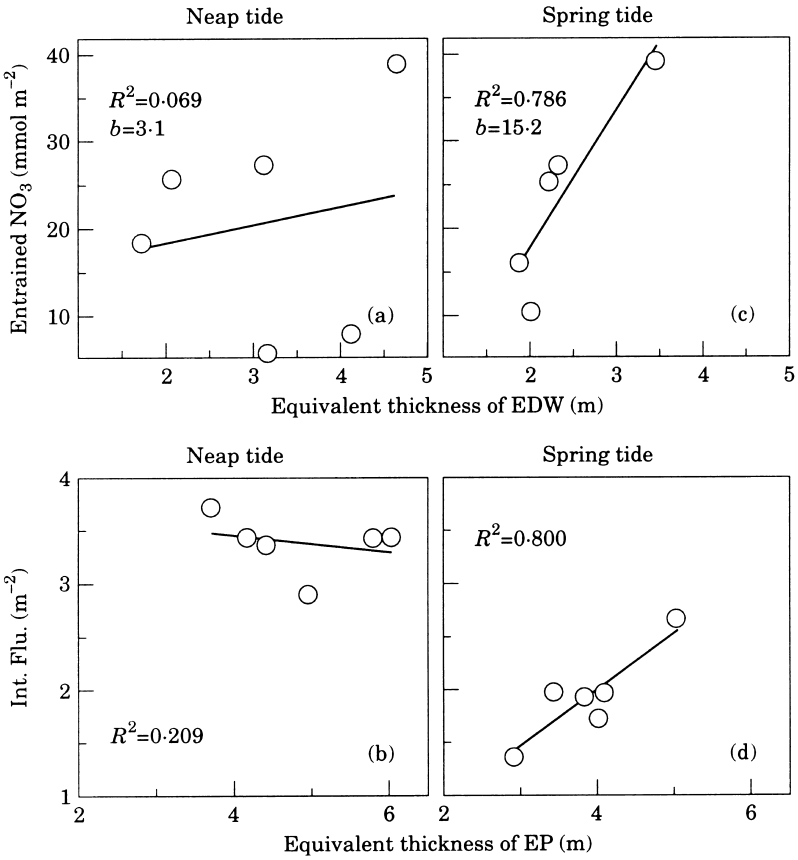

Figure 3. Linear regressions between the amount of the entrained NO_3 and the equivalent thickness of the entrained deep water (EDW) (a,c) and the depth-integrated fluorescence (Int. Flu.) and the equivalent thickness of the estuarine plume (EP) (b,d) for the neap tide of 12–13 June and the spring tide of 19–20 June 1989. The slopes of (a) and (c) are indicated by *b*. T1, T2 and T5 are not included in the regression in (c) because NO_3 concentrations were not measured, or were not deep enough for the calculation of entrained NO_3. T1 and T5 are not included in the regression in (d) for the same reason.

[Figure 1(b)]. There was a large NO_3 gradient between 22.00 and 24.00h at 10–25 m during HHW. A NO_3 minimum was observed at an intermediate depth (9 m) during almost the entire period [Figure 1(b)].

The amount of the entrained NO_3 varied greatly over the tidal cycle [Figure 3(a)]. Regression analysis indicated that there was no significant relationship between the amount of entrained NO_3 and the entrained deep water [R^2=0·07; Figure 3(a)], or between the depth-integrated fluorescence and the equivalent thickness of the estuarine plume [R^2=0·21; Figure 3(b)].

Spring tide

The surface salinity was <15 during the entire period and <10 at the end of time series (02.00–09.00h), indicating the presence of the riverine plume [Figure 1(c)]. The isohaline of 28 fluctuated between 13 m at LLW and 6 m at HHW.

Figure 2(b) shows the time series of T-S diagrams. At T2, temperature dropped initially in the left part of the curve [Figure 2(b)], representing the entrained colder water in the riverine plume. The hollow of the kink that was seen during the neap tide became larger (T4, T5 and T6), suggesting more entrainment of the deep water into the riverine plume. Temperature at the kink dropped by almost 1 °C during the spring tide from that during the neap tide.

The surface NO_3 concentrations [Figure 1(d)] remained at about 7 μM during the larger flood and at HHW (13.00–19.00h), and lower higher water (LHW) (04.00h). Compared with the NO_3 concentration of 6·8 μM in the river, these values indicate entrainment of NO_3. Because the surface salinity had increased to about 10, NO_3 in the riverine plume would be less than 6·8 μM if freshwater was mixed with the estuarine plume in which NO_3 concentrations were even lower. The surface NO_3 concentration dropped to below 2 μM during the smaller ebb (21.00–01.00h). The NO_3 contour lines (8–12 μM) at the intermediate depths oscillated with tidal height, rising during the larger flood (13.00–16.00h) and moving downwards during the next ebb. A depth minimum in NO_3 concentration was absent during the time series except near the end (06.00–09.00h). Several processes could cause the erosion of the NO_3 minimum. When the NO_3 concentration was 7 μM at the surface, the erosion was caused by the direct entrainment of the deep water by the riverine plume as can be seen at T3 and T7 in the T-S diagrams [Figure 2(b)] where the estuarine plume was not a distinct water mass. When the surface NO_3 concentration was below 2 μM, the absence of the minimum was simply due to no increase in the NO_3 concentration at the surface.

The amount of the entrained NO_3 varied over time but was dependent on the amount of the entrained deep water. Regression analyses showed that the entrained deep seawater accounted for 79% of the amount of entrained NO_3 [Figure 3(c)]. Similarly, the equivalent thickness of the estuarine plume explained 80% of the depth-integrated fluorescence [Figure 3(d)].

Comparison between the neap and the spring tides

A summary of the comparison between the spring and neap tides is shown in Table 1. Since the wind speed and the river discharge were similar, the differences in time-averaged parameters were apparently due to the difference in the tidal ranges, 4·0 m for the spring tide and 2·5 m for the neap tide. The equivalent thickness of the entrained estuarine plume was 1·6 m during the spring tide, whereas it was 2·8 m during the neap tide. The amount of entrained NO_3 was higher (24 mmol m^{-2}) for the spring than for the neap tide (17 mmol m^{-2}), although the amount of the entrained deep seawater was similar. The contribution of the entrained NO_3 relative to the river-borne NO_3 was greater for the spring (2·3) than for the neap tide (1·6), although the ratio of the entrained deep water to freshwater was almost the same (2·7). In contrast, the depth-integrated fluorescence was higher during the neap than during the spring tide.

Effects of river discharge

Lower discharge

The average river discharge during 29–30 May was 6720 m^3 s^{-1}. The surface salinity was <15 during most of the time series [Figure 4(a)]. It seems that the riverine plume frequently moved over the station, being more apparent in the beginning at LHW and the end at HLW. During these times, the gradients in the isohalines were also greater. The isohaline of 28 did not fluctuate much.

TABLE 1. Comparisons between the neap tide on 12–13 June and the spring tide on 19–20 June 1989. All the parameters are time-averaged over the time series

Parameter	Neap tide	Spring tide
Sampling period (h)	22·65	22·55
Tidal range (m)	2·5	4·0
Mean tidal height (m)	3·0	3·2
Wind speed ($m\ s^{-1}$)	3·7[a]	2·8[b]
Discharge ($m^3\ s^{-1}$)	6670	6850
Equivalent thickness (m)		
Freshwater	1·6	1·4
Entrained estuarine plume (EEP)	2·8	1·6
Entrained deep seawater (EDW)	3·0	2·9
Freshwater-penetration depth (m)	7·3	5·8
Entrained NO_3 ($mmol\ m^{-2}$)	17·3	24·2
River-borne NO_3 ($mmol\ m^{-2}$)	10·6	9·6
Depth-integrated fluorescence (m^{-2})	3·4	1·9
Ratio of sum of EEP and EDW to freshwater	3·7	3·2
Ratio of EDW to freshwater	1·9	2·0
Ratio of entrained NO_3 to river-borne NO_3	1·6	2·3

[a]Winds from the east were dominant.
[b]Winds fluctuated but were predominantly from the east.

The NO_3 concentrations in the top 3 m were low (<4 μM) in the first 7 h during the large ebb and remained higher than 6 μM) during the flood and the next small ebb. Particularly during HHW, the NO_3 concentrations were 8·9 μM [Figure 4(b)] which were higher than the river NO_3 concentration (7·5 μM), indicating entrainment of NO_3 into the riverine plume. Below these higher NO_3 concentrations, two NO_3 minima were present and very low at times [almost 0 μM, e.g. the two sets of circular contour lines between 21.00 and 23.00h in Figure 4(b)]. The features of the NO_3 contour plot are consistent with the T-S curves in the time series [Figure 5(a)]. At T1, T2 and T3, the estuarine plume was relatively dominant and the NO_3 concentrations were low. The drop in temperature at a salinity of 25 at T4 [Figure 5(a)] indicates mixing with the colder deep water by entrainment. At T7 [Figure 5(a)], the top part of T-S curve bent horizontally, suggesting that the estuarine plume was pushed seaward by the riverine plume, and the NO_3 concentration started to increase [Figure 4(b)]. As a result, the NO_3 minimum disappeared [Figure 4(b)]. The amount of entrained deep water accounted for 89% of the entrained NO_3 [Figure 6(a)]. The slope of the regression was 16·8 μM which was actually the average concentration of source NO_3 to be entrained. The estuarine plume accounted for 68% of the depth-integrated fluorescence in the water column [Figure 6(a)]. The time-averaged amount of the entrained NO_3 during the tidal cycle was 32 $mmol\ m^{-2}$ (Table 2).

Higher discharge

The river discharge increased to 9000 $m^3\ s^{-1}$ by 7 June 1990 and the tidal cycle was similar to the 29–30 May time series [Figure 4(c)]. The low surface salinities indicated that the riverine plume occupied the surface of the water column during most of the tidal cycle. The isohaline of 28 fluctuated with the tidal height. The isohalines (10–28) were deeper (07.00–08.00h) and became wider spaced during the large ebb (08.00–10.00h).

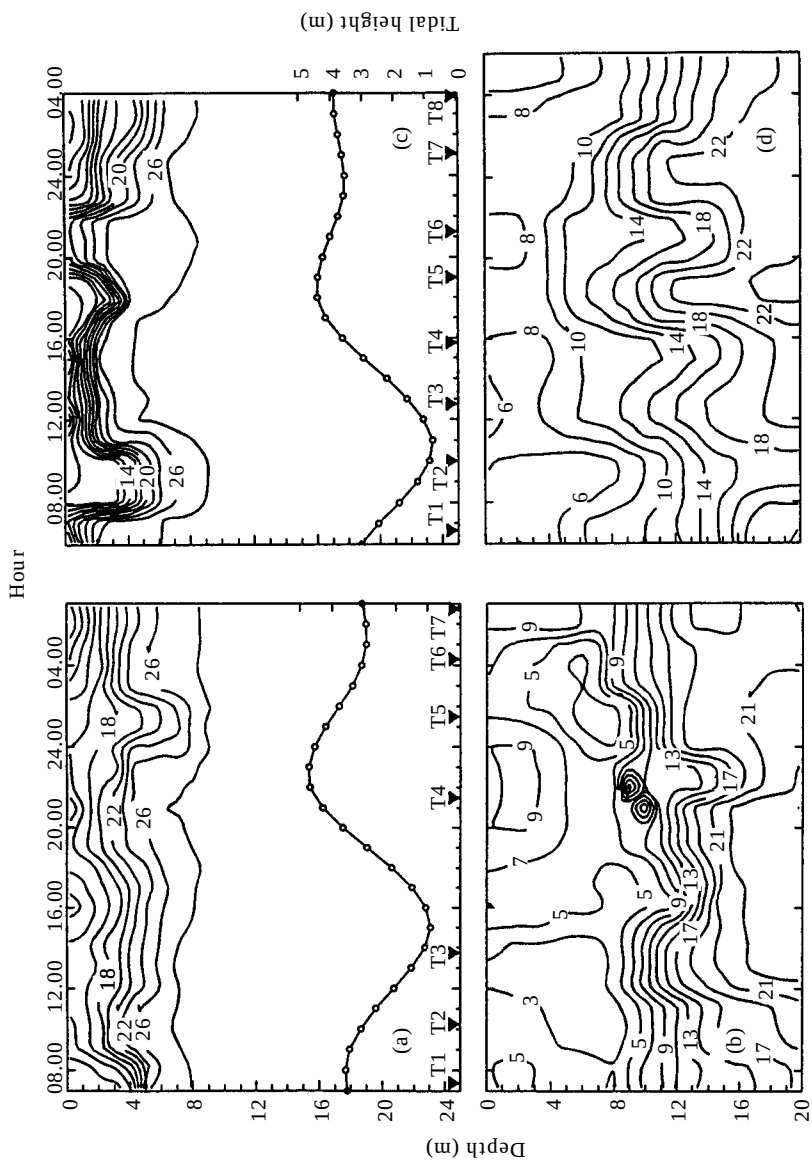

Figure 4. Depth contours of (a,c) salinity and (b,d) NO_3 (μM) for the time series at station 2 on 29–30 May during a day of lower river discharge (a,b) and on 7–8 June 1990 during a day of higher river discharge (c,d). The contours in (a) and (b) were plotted using more vertical profiles than the arrows indicated. Those arrows indicate only the sampling times (when the vertical profiles were completed) for the time series of T-S diagrams and the equivalent thickness shown in Figures 6(a) and 7(a). Therefore, the contours in (a) and (b) present more features than the number of the vertical profiles indicated by the arrows (for example, around T4 when another vertical profile with a NO_3 minimum at an intermediate depth is contoured close to T4 in time, two sets of circular contour lines next to each other are formed). The x-axis for the NO_3 contour in (d) is longer than in (c), because the salinity instrument for the last vertical profile was broken and not plotted in (d).

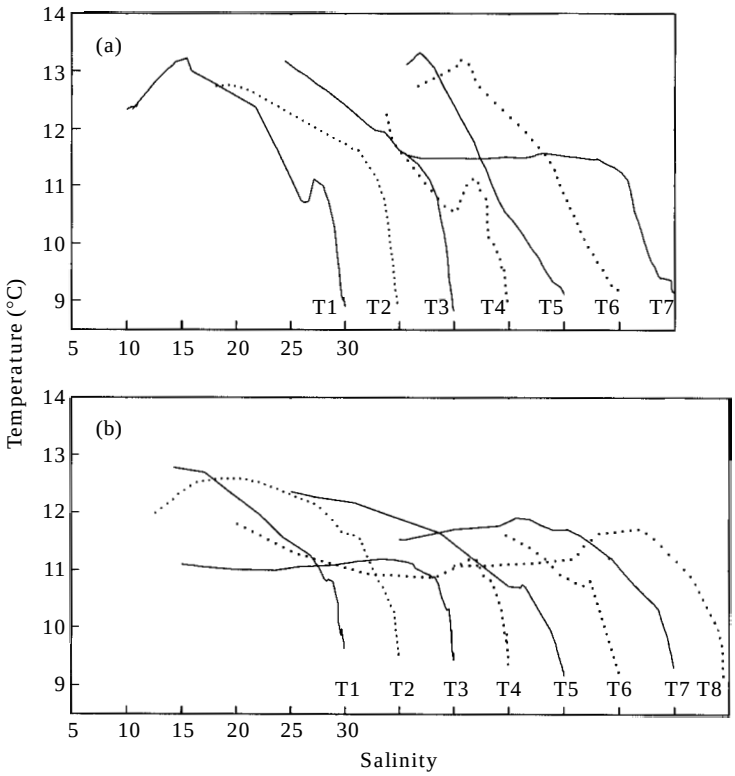

Figure 5. Time series of the T-S diagrams for (a) the smaller discharge on 29–30 May and (b) the larger discharge on 7–8 June 1990. See Figure 5(a) for the sampling times. Successive T-S curves are offset by 5 on the salinity axis.

During the following flood (10.00–16.00h), however, the isohalines became shallower and the gradient increased [Figure 4(c)].

Surface NO_3 concentrations remained nearly constant at 6–8 μM [Figure 4(d)]. The most pronounced feature in the contour plot was the absence of the NO_3 minimum. The estuarine plume was no longer a distinct water mass in the water column, as indicated in the T-S diagrams [Figure 5(b)]. The left segments of the T-S lines were bent more horizontally than ones on 29–30 May, and generally, temperatures on the bent line segments were lower than ones for the same salinities on the T-S diagrams of the 29–30 May series. The kinks were nearly absent. The regression analysis indicated that the amount of the entrained deep seawater accounted for 82% of the amount of entrained NO_3 and the slope was 25 μM [Figure 6(c)]. Similarly, the depth-integrated fluorescence was strongly determined by the equivalent thickness of the estuarine plume [$R^2 = 0{\cdot}975$; Figure 6(d)].

Table 2 shows a summary comparison between the two time series. The equivalent thickness of the freshwater was thicker for the larger discharge than for the smaller one, indicating that the riverine plume occupied the station more frequently and/or was more pronounced. The amount of the entrained NO_3 during the higher discharge was (73 mmol m^{-2}), twice as much as during lower discharge. The contribution of the entrained NO_3 relative to the river-borne NO_3 increased to 5·4 from 3·3 for the

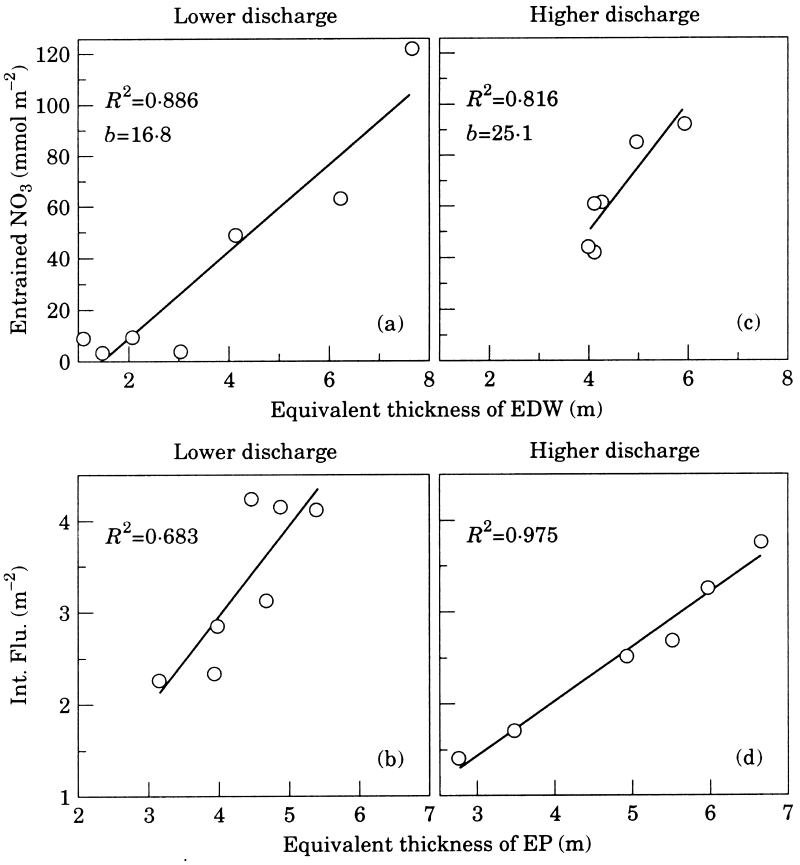

Figure 6. Linear regressions between the amount of the entrained NO_3 and the equivalent thickness of the entrained deep water (EDW) (a,c) and the depth-integrated fluorescence (Int. Flu.) and the equivalent thickness of the estuarine plume (EP) (b,d) for the low discharge on 29–30 May and the higher discharge on 7–8 June 1990. The slopes of (a) and (b) are indicated by *b*. T5 and T6 are not included in the regression in (c) and (d) for the same reason as stated in Figure 7.

lower discharge. The fluorescence in the water column decreased during the larger discharge.

Discussion

Spring vs. *neap tides*

In the Strait of Georgia, the differences in tidal range depend on the change in LLW during the tidal cycle. More of the river discharge entered the Strait during the spring ebb of 19 June than during the neap ebb of 12 June because the water level in the strait was 2 m lower at LLW during the spring tide, even though the amount of river discharge was almost the same between the two tidal cycles. Furthermore, during the subsequent spring flood on 19 June, the river outflow and the rising water levels squeezed the estuarine plume in the middle. As a result, the salinity gradients were greater and the estuarine plume was thinner during the spring tide. A similar process has been

TABLE 2. Comparisons between the low discharge on 29–30 May and the higher discharge on 7–8 June 1900. All the parameters are time-averaged over the time series

Parameters	Lower discharge	Higher discharge
Sampling period (h)	23·4	22·6
Tidal range (m)	3·9	3·7
Mean tidal height (m)	3·2	3·2
Wind speed ($m\ s^{-1}$)	3·4[a]	2·7[b]
Discharge ($m^3\ s^{-1}$)	6720	9000
Equivalent thickness (m)		
Freshwater	1·3	1·8
Entrained estuarine plume (EEP)	2·7	3·0
Entrained deep seawater (EDW)	3·4	4·8
Freshwater-penetration depth (m)	7·4	9·6
Entrained NO_3 ($mmol\ m^{-2}$)	31·7	72·3
River-borne NO_3 ($mmol\ m^{-2}$)	9·5	13·5
Depth-integrated fluorescence (m^{-2})	3·4	2·5
Ratio of sum of EEP and EDW to freshwater	4·7	4·3
Ratio of EDW to freshwater	2·7	2·7
Ratio of entrained NO_3 to river-borne NO_3	3·3	5·4

[a]Winds from east were dominant.
[b]Winds fluctuated and were from the east or south.

demonstrated in a laboratory experiment by Nof (1979) who showed that the middle layer decreased its thickness when a surface layer flowed from one end and a bottom layer invaded at the other end of the water tank. Nitrate concentrations in the deep water were higher, as indicated by the steeper slope of the regression (Figure 3) between the amount of the entrained NO_3 and the entrained deep water because of stronger bottom stirring during the spring tide. Particularly in the region at the river mouth where the bottom depth rapidly decreases toward the river mouth, higher concentrations of NO_3 would be mixed upward into the salinity wall near the mouth, or into the salt wedge and exposed to the riverine plume (Figure 7). In fact, NO_3 concentrations in the lower part (below 12 m) of the water column were higher during the spring tide than during the neap tide [Figure 1(b,d)]. As a result, there was more entrained NO_3 during the spring tide, although the amount of the entrained deep seawater during the spring tide was not greater. The ratio of the contribution of the entrained NO_3 to the surface layer relative to the river-borne NO_3 during the spring tide was greater than during the neap tide, although the ratios of entrained deep seawater to freshwater were very similar (Table 1). Also, because of the stronger mixing during the spring tide, the amount of entrained NO_3 was more dependent on the amount of entrained deep seawater and the depth-integrated fluorescence decreased, and was more closely related to the estuarine plume than during the neap tide. The lack of a relationship between the entrained NO_3 and the entrained deep seawater during the neap tide might be due to two reasons. One is that the deep seawater contained different NO_3 concentrations, as seen in the NO_3 contour plot [Figure 1(b)] where NO_3 contour lines below 12 m had lower values during the later part of the time series during the neap tide. The other reason is that mixing was slow and the mixture of the water masses during the neap tide had been there for a sufficiently long time for NO_3 to be consumed. This idea is supported by higher chlorophyll in the water column indicated by the greater depth-integrated fluorescence

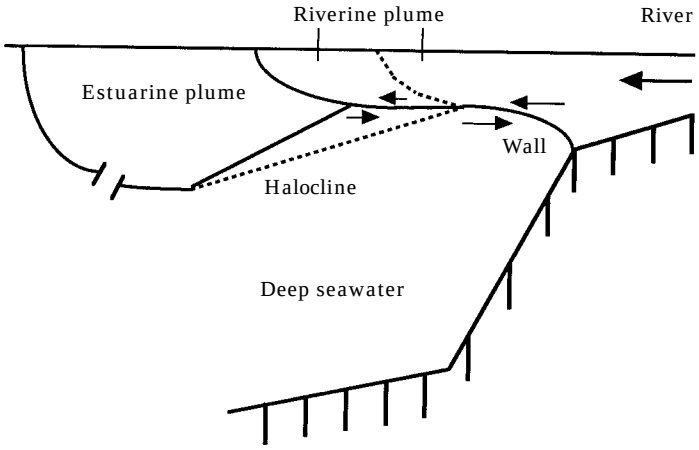

Figure 7. The conceptual model illustrating how the wall (the area of the deep seawater exposed to the riverine plume seaward of the river mouth) changes with the riverine plume, the estuarine plume and the deep water during different stages of tidal cycles and river discharge. The dashed line indicates a condition during a neap ebb or smaller discharge and the solid line indicates a spring ebb or larger discharge condition.

and no significant relationship between the equivalent thickness of the estuarine plume and the integrated fluorescence, compared with a significant relationship for the spring tide.

It appears that there can be a fortnightly tidal cycle in nutrient mixing and phytoplankton biomass in the estuarine plume. During a spring tide, phytoplankton biomass could be reduced (by dilution) and nutrient mixing could be increased. After the spring tide, the tide-induced mixing processes would slow down and the estuarine plume would increase in thickness possibly by wind mixing of the remnants of the old riverine plume. Supplied nutrients could be taken up with a subsequent increase in phytoplankton biomass. During an approaching neap tide, a bloom might develop, resulting in a higher fluorescence (e.g. Table 1) and lower NO_3 concentrations in the source water which could be entrained during the neap tide. A pre-neap tide bloom has been observed by Harrison *et al*. (1991) for the same region in July.

Higher vs. *lower river discharge*

The time series on 29–30 May and 7–8 June 1990 were during similar tidal ranges, close to the spring tide, with similar low average wind speeds. Thus, a comparison between the two time series to examine the effects of river discharge is possible. Furthermore, the discharge of 9000 $m^3\ s^{-1}$ on 7 June had been preceded by 4 days of higher discharge that were near the annual maximum (10 100 $m^3\ s^{-1}$). Therefore, the results of this study also represent the interaction between the maximum river discharge and the biggest spring tide of the year and its effects on entrainment as well as the water column structure.

It appears that the discharge on 7–8 June was so strong that the estuarine plume was swept seaward and the area at the wall extended much farther into the Strait beyond the river mouth than during the small discharge condition (Figure 7). As a result, the NO_3 minimum in the contour was absent [Figure 4(d)]. Also, the freshwater penetrated deeper into the water column, 9·6 m compared with 7·4 m for the smaller discharge on

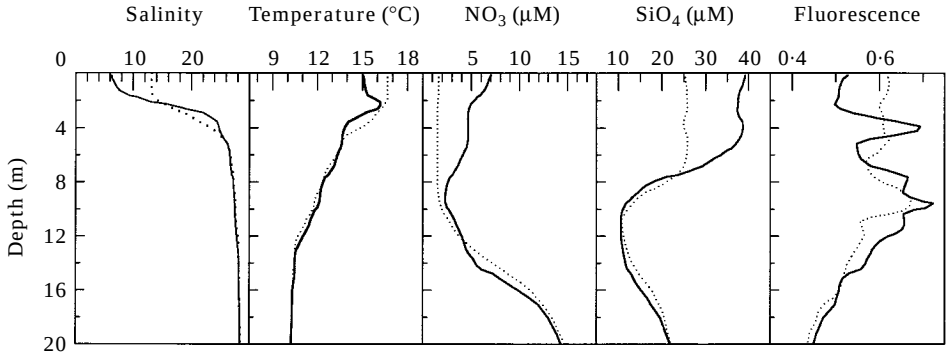

Figure 8. A riverine front (shown in Figure 7) crossed a station, 35 km away from the river mouth on 14 June 1989. Two vertical profiles were taken within 30 min, one (· · · ·) was 50 m away from the riverine front (seaward of the riverine plume) and the other (——) after the riverine front passed the station 20 m away (within the riverine plume). The movement of the riverine front induced entrainment of NO_3 and produced double chlorophyll *a* maxima.

29–30 May (Table 2). This deeper penetration of the riverine plume allowed it to contact the higher NO_3 concentrations indicated by the higher slope (25 μM) over the large area. As a result, more NO_3 (72 mmol m^{-2}) was entrained during higher discharge, about twice as much (32 mmol m^{-2}) as during lower discharge. The entrained NO_3 contribution to the surface layer was five times the river NO_3 contribution, compared with three times for the smaller discharge on 29–30 May (Table 2). It is interesting to note that the ratios of entrained deep water to freshwater were the same between the two discharges. This was also the case between the spring and neap tides. It appears that any physical and biological processes that affect the source NO_3 concentration would affect the amount of the entrained NO_3 as well.

Entrainment and its biological significance

In previous studies, the fluorescence maximum was located at the interface between the estuarine plume and the deep water and coincided with the NO_3 minimum. The maximum is advected with the interface toward or into the river and phytoplankton are entrained into the riverine plume above the interface. Figure 8 demonstrates the entraining process that formed the double fluorescence maxima. One vertical profile (indicated by the dotted lines) was taken in the estuarine plume (i.e. seaward side of the riverine plume) 50 m away from the riverine front (see Figure 7). The other vertical profile (indicated by the solid lines) was taken 15 min after the riverine front crossed the anchored ship. While the deep layer remained very similar, the salinity in the surface layer decreased by 7 and the temperature decreased by more than 1 °C. The increase in the silicate concentration was another indicator of the presence of the riverine plume. Nitrate entrainment was evident from this cross-front vertical profile. More interesting is the formation of double fluorescence maxima when the riverine front crossed the station. The shallower one was located at the sharp halocline. Apparently it was entrained from the deep maximum and dragged along as the front advanced. The feature of the double chlorophyll maxima coinciding with the NO_3 concentration minima in the water column has been reported for the same area (Cochlan *et al.*, 1989). The double chlorophyll

maxima feature associated with the water flow was also reported for Chesapeake Bay (Tyler, 1984).

The entrained phytoplankton could be very important in seeding downstream in the estuary. In the lower St Lawrence estuary, the seeding of the fresher surface layer by entrainment of seed cells from the saline deeper layer is suggested to be of great importance in initiating the spring phytoplankton bloom (Therriault & Levasseur, 1986). A recent study in the Gulf of Maine applying temperature–salinity diagrams in the analysis of water masses, indicated that the colder nutrient-rich deeper waters of the slope origin contribute a significant fraction of the high nutrient concentrations (Townsend *et al.*, 1987). In the estuarine plume in the Strait of Georgia, the entrained phytoplankton would take up the entrained nutrients and grow faster because of the improved light conditions due to settling of suspended sediments as they move away from the river. A bloom should develop, forming a regional maximum of primary production in the estuarine plume. Previous studies in the Strait found a productivity maximum in the estuarine plume (Parsons *et al.*, 1969; Stockner *et al.*, 1979; Harrison *et al.*, 1991). Zooplankton appear to form a regional abundance maximum around this region (Parsons *et al.*, 1969; Mackas & Louttit 1988; St John *et al.*, 1992).

In summary, the process of entrainment starts in the Fraser River estuary and extents beyond the river mouth. Salt entrainment does not necessarily mean NO_3 entrainment. The amount of entrained NO_3 was accounted for by the entrained deep seawater (EDW) rather than the sum of EDW plus the entrained estuarine plume (EEP). Most upward entrainment occurred during tidal ebbs. More NO_3 was entrained during spring tides than neap tides. More NO_3 was entrained as river discharge increased. The contribution of entrained NO_3 from the deep water to the upper layer was 1·6–5·5 times the river-borne NO_3. Winds also play an important role in regulating entrainment processes (St John *et al.*, 1993). The wind effects will be further examined in next study (Yin *et al.*, 1995*b*).

Acknowledgements

We thank Dr Mike St John and Peter Clifford who coordinated the cruises and the following cruise participants; Robert Goldblatt and Heidi Sawyer. David Jones helped to set up the vertical profiling system. Thanks are given to the Department of Fisheries and Oceans for providing ship time, and the officers and crew of C.S.S. *Vector* for their assistance. Discussions with Dr Keith Thompson were helpful, and comments by Drs James Cloern, Ken Denman and Peter Franks improved the manuscript.

This research was funded by a Natural Sciences and Engineering Research Council of Canada (NSERC) Strategic grant. The Research Fellowship to support K. Yin was kindly provided by the Department of Fisheries and Oceans, Pacific Biological Station, Nanaimo, British Columbia, Canada.

References

Clifford, P. J., Cochaln, W. P., Harrison, P. J., Yin, K., Sibbald, M. J., Albright, L. J., St John, M. A. & Thompson, P. A. 1989 Plankton production and nutrient dynamics in the Fraser River plume, 1987. *Department of Oceanography, University of British Columbia Report* No. 51. 118 pp.

Clifford, P. J., Harrison, P. J., Yin, K., St John, M. A., Waite, A. M. & Albright, L. J. 1990 Plankton production and nutrient dynamics in the Fraser River plume, 1988. *Department of Oceanography, University of British Columbia Report* No. 53. 142 pp.

Clifford, P. J., Harrison, P. J., St John, M. A., Yin, K. & Albright, L. J. 1991 Plankton production and nutrient dynamics in the Fraser River plume, 1989. *Department of Oceanography, University of British Columbia Report* No. 54. 255 pp.

Cochlan, W. P., Harrison, P. J., Clifford, P. J. & Yin, K. 1989 Observation of double chlorophyll *a* maximum in the vicinity of the Fraser River plume. *Journal of Experimental Marine Biology and Ecology* **143,** 139–146.

Drinnan, R. W. & Clark, M. J. R. 1980 Water chemistry: 1970–1978. Fraser River Estuary Study, Water Quality Working Group, Ministry of Environment, Parliament Buildings, Victoria, B. C., 150 pp.

Harrison, P. J., Fulton, J. D., Taylor, F. J. R. & Parsons, T. R. 1983 Review of the biological oceanography of the Strait of Georgia: pelagic environment. *Canadian Journal of Fisheries and Aquatic Science* **40,** 1064–1094.

Harrison, P. J., Clifford, P. J., Cochlan, W. P., Yin, K., St John, M. A., Thompson, P. A., Sibbald, M. J. & Albright, L. J. 1991 Nutrient and phytoplankton dynamics in the Fraser River plume, Strait of Georgia, British Columbia. *Marine Ecology Progress Series* **70,** 291–30.4

Jones, D. M., Harrison, P. J., Clifford, P. J., Yin, K. & St John, M. A. 1991 A computer-based system for the acquisition and display of continuous vertical profiles of temperature, salinity, fluorescence and nutrients. *Water Research* **25,** 1545–1548.

Mackas, D. L. & Louttit, G. C. 1988 Aggregation of the copepod *Neocalanus plumchrus* at the margin of the Fraser River plume in the Strait of Georgia. *Bulletin of Marine Science* **43,** 810–824.

Nof, D. 1979 Generation of fronts by mixing and mutual intrusion. *Journal of Physical Oceanography* **9,** 298–310.

Parsons, T. R., LeBrasseur, R. J., Fulton, J. D. & Kennedy, O. D. 1969 Production studies in the Strait of Georgia. I. Primary production under the Fraser River plume, February to May, 1967. *Journal of Experimental Marine Biology and Ecology* **3,** 27–38.

Parsons, T. R., LeBrasseur, R. J. & Barraclough, W. E. 1970 Levels of production in the pelagic environment of the Strait of Georgia, British Columbia: a review. *Journal of the Fisheries Research Board of Canada* **27,** 1251–1264.

Parsons, T. R., Albright, L J. & Parslow, J. 1980. Is the Strait of Georgia becoming more eutrophic? *Canadian Journal of Fisheries and Aquatic Science* **37,** 1043–1047.

Rudek, J., H. W., Paerl, M. A. M. & Bates, P. W. 1991 Seasonal and hydrological control of phytoplankton nutrient limitation in the lower Neuse River estuary, North Carolina. *Marine Ecology Progress Series* **75,** 133–142.

St John, M. A., Macdonald, J. S., Harrison, P. J., Beamish, R. J. & Choromanski, E. 1992 The Fraser River plume: effects on the distribution of juvenile salmonids, herring and their prey. *Fisheries Oceanography* **1,** 153–162.

St John, M. A., Marinone, S. G., Stronach, J., Harrison, P. J., Fyfe, J. & Beamish, R. J. 1993 A horizontal resolving physical–biological model of nitrate fluxes and primary productivity in the Strait of Georgia. *Canadian Journal of Fisheries and Aquatic Science* **50,** 1456–1466.

Stockner, J. G., Cliff, D. D. & Shortreed, K. R. S. 1979 Phytoplankton ecology of the Strait of Georgia, British Columbia. *Journal of the Fisheries Research Board of Canada* **36,** 657–66.

Therriault, J.-C. & Levasseur, M. 1986 Freshwater runoff control of the spatio-temporal distribution of phytoplankton in the lower St. Lawrence estuary. In *The Role of Freshwater Outflow in Coastal Marine Ecosystems* (Skreslet, S., ed.). NATO ASI series Vol. G7. Springer-Verlag, Berlin.

Townsend, D. W., Christensen, J. P., Stevenson, D. K., Graham, J. J. & Chenoweth, S. B. 1987 The importance of a plume of tidally-mixed water to the biological oceanography of the Gulf of Maine. *Journal of Marine Research* **45,** 699–728.

Tyler, M. A. 1984. Dye tracing of a subsurface chlorophyll maximum of a red-tied dinoflagellate to surface frontal regions. *Marine Biology* **78,** 285–300.

Yin, K., Harrison, P. J., Pond, S. & Beamish, R. J. 1995*a* Entrainment of nitrate in the Fraser River estuary and its biological implications. I. Effects of the salt wedge. *Estuarine, Coastal and Shelf Science* **40,** 505–528.

Yin, K., Harrison, P. J. Pond, S. & Beamish, R. J. 1995*b* Entrainment of nitrate in the Fraser River estuary and its biological implications. III. Effects of winds. *Estuarine, Coastal and Shelf Science* **40,** 545–558.